

# Dynamical behavior of one-dimensional water molecule chains in zeolites: Nanosecond time-scale molecular dynamics simulations of bikitaite

Pierfranco Demontis, Giovanna Stara, and Giuseppe B. Suffritti<sup>a)</sup>

*Dipartimento di Chimica, Università degli studi di Sassari, and Consorzio Interuniversitario Nazionale per la Scienza e Tecnologia dei Materiali (INSTM), Unità di ricerca di Sassari, Via Vienna, 2, 07100 Sassari, Italy*

(Received 23 May 2003; accepted 16 February 2004)

Nanosecond scale molecular dynamics simulations of the behavior of the one-dimensional water molecule chains adsorbed in the parallel nanochannels of bikitaite, a rare lithium containing zeolite, were performed at different temperatures and for the fully and partially hydrated material. New empirical potential functions have been developed for representing lithium–water interactions. The structure and the vibrational spectrum of bikitaite were in agreement both with experimental data and Car–Parrinello molecular dynamics results. Classical molecular dynamics simulations were extended to the nanosecond time scale in order to study the flip motion of water molecules around the hydrogen bonds connecting adjacent molecules in the chains, which has been observed by NMR experiments, and the dehydration mechanism at high temperature. Computed relaxation times of the flip motion follow the Arrhenius behavior found experimentally, but the activation energy of the simulated system is slightly underestimated. Based on the results of the simulations, it may be suggested that the dehydration proceeds by a defect-driven stepwise diffusion. The diffusive mechanism appears as a single-file motion: the molecules never pass one another, even at temperatures as high as about 1000 K, nor can they switch between different channels. However, the mean square displacement (MSD) of the molecules, computed with respect to the center of mass of the simulated system, shows an irregular trend from which the single-file diffusion cannot be clearly evidenced. If the MSDs are evaluated with respect to the center of mass of the molecules hosted in each channel, the expected dependence on the square root of time finally appears. © 2004 American Institute of Physics. [DOI: 10.1063/1.1697382]

## I. INTRODUCTION

The confinement of water in porous media, in biological as well as in organic and inorganic materials, is an important phenomenon which has recently received a renewed interest, both from experimental and theoretical viewpoints. The literature in this field is so abundant<sup>1,2</sup> that it is not possible to report even the most outstanding publications without filling pages in the References section. Therefore, we shall limit ourselves to some recent examples. For instance, experimental evidence of possible phase transitions of supercritical liquid water at low temperatures has been looked for in hydrated phyllosilicates,<sup>3–6</sup> where the confinement would prevent nucleation, while new statistical models have been developed for studying the phases of water-like liquids in porous media.<sup>7–9</sup> Among the different approaches, the molecular dynamics (MD) simulation technique seems to be very promising in order to gain a better microscopic description for the behavior of water in porous materials.<sup>10–14</sup> A recent example is the study of the phase transitions of water in slit pores.<sup>15</sup> An extreme case of confined water is one-dimensional water chains, which are present in some zeolites like bikitaite,<sup>16</sup> whose study has been performed<sup>17–21</sup> by using the Car–Parrinello MD (CPMD) first principles method.<sup>22</sup> Presently, the computational cost of this very ef-

fective method is prohibitively high if the size of the system and the time scale to cover are large. The aim of this paper is to explore phenomena in a range where the relevant length and time scales are of the order of nanometers and tens of nanoseconds in order to give a further contribution to the understanding of the behavior of chains of water molecules in restricted geometries. For this reason we used classical molecular dynamics, and under this point of view our results could be considered as complementary to CPMD simulations.

Bikitaite<sup>16</sup> is of special interest because it shows parallel straight channels where hydrogen-bonded linear chains of water molecules run along the axis of the channels, parallel to regular rows of lithium ions sticking to the channel surface (see Fig. 1).

Whereas at low temperature the water molecule chains remain stable, although showing relatively large libration amplitudes around the hydrogen bonds, in the temperature range 224–418 K flips of the molecules, exchanging the hydrogen atoms, were observed in bikitaite by NMR experiments.<sup>23</sup> Relaxation times for flip motion in the range  $10^{-7}$  s (224 K)– $10^{-10}$  s (418 K) were observed, without any evident diffusion, even at the highest temperature.

On the other hand, recent x-ray diffraction experiments at high temperature<sup>24,25</sup> showed that at about 375 K the dehydration process begins and the complete dehydration is achieved at about 725 K. The seeming discrepancy between

<sup>a)</sup>Electronic mail: pino@uniss.it

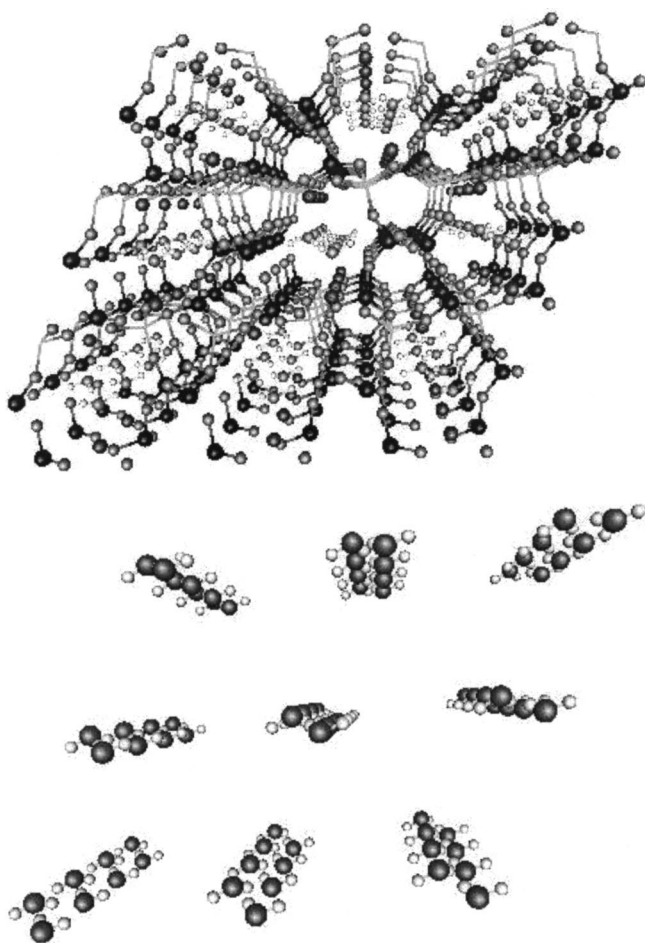


FIG. 1. The structure of bikitaite as seen from the crystallographic axis  $b$ . Top: the complete structure is represented; bottom: the water molecules chains only are displayed.

x-ray and NMR results can be explained by considering the different observation time, which is much smaller for NMR, so that very slow diffusive motion could have escaped in fitting NMR data.

In order to study these phenomena, in the present work classical MD simulations of water in bikitaite<sup>16</sup> extended to the nanosecond scale were performed. New empirical potentials for Li–zeolite and Li–water interactions were developed, and a sophisticated electric field-dependent model for flexible water was adopted. In the fully hydrated material the flip motion of water molecules was reproduced, and the relaxation times at different temperatures were evaluated. Even at the highest temperature (800 K) no diffusion was detected, indicating that, at least with the adopted model, energy barrier for water molecules to pass each other with full loading is much higher than  $k_B T$ . Preliminary results are reported in Ref. 13. In order to explain the experimentally observed dehydration process, it may be suggested that, in real (finite) crystals water can escape from the free ends of the channels, inducing a defect-driven stepwise diffusion, which eventually leads to dehydration. Therefore, partially dehydrated bikitaite was simulated in order to elucidate the diffusive mechanism, which indeed appears to be rather complex. The diffusive mechanism appears as a single-file motion: the molecules never pass one another, even at temperatures as

high as about 1000 K, nor can they switch between different channels. However, the mean square displacement (MSD) of the molecules, computed with respect to the center of mass of the simulated system, shows an irregular trend from which the single-file diffusion mechanism cannot be clearly evidenced. If the MSDs are evaluated with respect to the center of mass of the molecules hosted in each channel, the expected dependence on the square root of time finally appears.

## II. MODEL AND CALCULATIONS

Bikitaite<sup>16</sup> is a rare natural zeolite with 100% Li extra framework cations. Its chemical formula is  $\text{Li}(\text{AlSi}_2\text{O}_6)\text{H}_2\text{O}$ . The symmetry group of the crystal is  $P1$  with cell dimensions  $a=0.85971$ ,  $b=0.49395$ ,  $c=0.76121$  nm,  $\alpha=89.90^\circ$ ,  $\beta=114.52^\circ$ ,  $\gamma=89.99^\circ$ . The structure is characterized by parallel straight channels running along the  $b$  direction, delimited by 8-membered rings of  $(\text{Al,Si})\text{O}_4$  tetrahedra, where the water molecules are hydrogen bonded to each other and form one-dimensional chains parallel to the channel axis. Li cations are coordinated to three oxygen atoms of the framework and one water molecule, whose bisector is roughly perpendicular to the Li–O distance.

Standard MD simulations with periodic boundary conditions and in the microcanonical ensemble were performed for a system consisting of  $3 \times 4 \times 3$  unit cells of bikitaite (936 atoms) resulting in a simulation box of sides  $a'=2.57913$ ,  $b'=1.9758$ ,  $c'=2.28363$  nm, forming the same angles as above reported. This choice is a compromise between the requirement of simulating a system as large as possible to study the diffusion of the water molecules and of a reasonable computer time. Indeed, even using empirical potentials and an efficient method to evaluate the unavoidable Coulombic interactions (see below), a typical run lasting some nanoseconds required some hundreds of hours of computer time on a Compaq DS20 UNIX workstation. The full hydration of the crystal corresponds to 72 molecules per simulation box. Partially dehydrated bikitaite was obtained by removing one or more molecules per channel. The channels were 9 per simulation box. As mentioned in the Introduction, a sophisticated empirical model for simulating flexible water molecules<sup>12</sup> was adopted. Its intramolecular part was fitted to an MRSDCI potential energy surface including 37 configurations of the water molecule, some of them very far from the equilibrium geometry.<sup>26</sup> A polynomial fit of this surface around the minimum energy geometry, reported in Ref. 26, as well as a more sophisticated fit to all the considered configurations performed in this laboratory,<sup>27</sup> yielded a very good reproduction of both experimental geometry and vibrational frequencies. The intramolecular potential of water was further implemented, by adding terms depending on the electric field acting on the molecule, in order to reproduce the deformations and the frequency shifts shown by the water molecules in an environment where an electric field is present.<sup>12</sup> This model was completed with the intermolecular part, and the final form and parameters are reported in Ref. 12. To include lattice vibrations and deformations in the simulated system, a flexible zeolite framework model developed in this laboratory<sup>14,28</sup> has been used. Moreover, new

TABLE I. Values of the parameters included in Eqs. (1)–(4). Energies are obtained in kJ/mol if the distances are in units of  $10^{-10}$  m (formerly Å).

Interaction	A	B	C	$\sigma$		
Li <sup>+</sup> –O	$2.68 \times 10^5$	5.15	397.2	0.5		
Li <sup>+</sup> –H	$4.14 \times 10^7$	7.07	410.8	0.5		
O–O <sub>w</sub>	$8.36 \times 10^5$	3100	209	...		
O–H <sub>w</sub>	2090	179.9	...	...		
Li <sup>+</sup> –O	$6.276 \times 10^6$	5.5	...	...		
Charges	$q_{\text{Li}^+}/e$	$q_{\text{O}}/e$	$q_{\text{H}}/e$	$q_{\text{O}_f}/e$	$q_{\text{Si}}/e$	$q_{\text{Al}}/e$
	1.0	-0.659 66	0.329 83	-1.0	1.825	1.35

empirical potential functions have been elaborated to represent Li<sup>+</sup>–water interactions, as the ones previously proposed for simulating aqueous solutions containing lithium ions did not reproduce the structure of water in bikitaite.

Indeed, water molecules are located in planes which are roughly *perpendicular* to the Li–O distance, whereas for all previously available empirical Li<sup>+</sup>–water potential models the preferred orientation of water molecule was *parallel* to this distance, with high barrier to flap motion. The special features of Li<sup>+</sup>–water interactions were recently discussed by Lyubartsev *et al.*<sup>29</sup> in an *ab initio* MD simulation study of lithium salt aqueous solutions. Therefore, a new model fitting both *ab initio* results<sup>30–34</sup> for the Li<sup>+</sup>–water system and experimental data for bikitaite was performed. The final form of the Li<sup>+</sup>–water potential function reads

$$V_{\text{LiO,H}}(r) = \frac{1}{4\pi\epsilon_0} \frac{q_{\text{Li}}q_{\text{O,H}}}{r} + A_{\text{LiO,H}} \exp(-b_{\text{LiO,H}}r) + \frac{C_{\text{LiO,H}}}{r^2} S(\sigma, r), \quad (1)$$

where  $S(\sigma, r)$  is a switching function given by

$$S(\sigma, r) = \begin{cases} 1 & \text{if } r < 0.5 \text{ nm} \\ \exp(-\sigma r^2) & \text{if } r \leq 0.5 \text{ nm}, \end{cases} \quad (2)$$

which is necessary because the  $r^{-2}$  lattice sums do not converge, as in Eq. (1)  $C_{\text{LiO}} \neq -2C_{\text{LiH}}$ .

The values of the parameters are reported in Table I, and the optimized quantities of the isolated Li<sup>+</sup>–H<sub>2</sub>O system are compared with the *ab initio* results<sup>30–34</sup> in Table II.

As in our previous papers,<sup>12–14</sup> water was assumed to interact with Si and Al atoms via a Coulomb potential only, and the potential functions between the oxygen atoms of the

TABLE II. Optimized Li–O distance and interaction energy for the isolated Li<sup>+</sup>–H<sub>2</sub>O system according to the empirical potential derived in this work and to *ab initio* calculations.

	Li <sup>+</sup> –O (nm)	Interaction energy (kJ/mo)
This work	0.185	-140.5
Ref. 26	0.185	-157.7
Ref. 27	0.185	-166.1
Ref. 28	0.185	-166.1
Ref. 29	0.182	-148.9
Ref. 30	0.184	-152.7

framework and the oxygen or hydrogen atoms of water were derived from a simplified form of the corresponding O–O and O–H ones for water–water interactions.

The potentials for interactions between an oxygen atom of the zeolite framework (O<sub>f</sub>) and an oxygen (O) or a hydrogen (H) atom of the water molecule were represented by

$$V_{\text{O}_f\text{O}} = \frac{1}{4\pi\epsilon_0} \frac{q_{\text{O}_f}q_{\text{O}}}{r} + \frac{A}{r^{12}} - \frac{B}{r^6} + \frac{C}{r^4}, \quad (3)$$

$$V_{\text{O}_f\text{H}} = \frac{1}{4\pi\epsilon_0} \frac{q_{\text{O}_f}q_{\text{H}}}{r} + \frac{A}{r^7} - \frac{B}{r^4}. \quad (4)$$

The values of the refined parameters are collected in Table I. These parameters are different from the ones reported in Ref. 12, where only structural data of natrolite, a natural zeolite,<sup>35</sup> were fitted.

Finally, for the interactions between Li<sup>+</sup> and Si and Al atoms of a simple Coulomb potential was considered, and the potential functions between Li<sup>+</sup> and the oxygen atoms of the framework were represented by

$$V_{\text{LiO}_f}(r) = \frac{1}{4\pi\epsilon_0} \frac{q_{\text{Li}}q_{\text{O}_f}}{r} + A_{\text{LiO}_f} \exp(-b_{\text{LiO}_f}r). \quad (5)$$

The values of the parameters are reported again in Table I. The evaluation of the Coulomb energy was performed by using the efficient method recently proposed by Wolf *et al.*<sup>36</sup> and extended in our laboratory to complex systems.<sup>37</sup> The cutoff radius was  $R_C = 1.837$  nm, equal to one half of the largest diagonal of the simulation box, and, correspondingly, the damping parameter was  $\alpha = 2/R_C = 2.017 \text{ nm}^{-1}$ .

Runs lasting, after equilibration, 0.04–11 ns (using a time step of 0.5 fs) were carried out at low temperature (about 50 K) and at room temperature, in order to compare the structural results with the available experimental spectroscopic and structural data, and then at higher temperatures (in the range 420–1000 K) to check the mobility of the water molecules. In Table III the main characteristics of the simulations are collected. The duration of the simulation was longer for smaller concentrations, in order to obtain evenly good statistics. Some trajectories were prolonged to verify the trend of the results at longer times.

Besides structural properties (average coordinates, radial distribution functions, and distribution profiles along the channels), the vibrational spectrum and the time autocorrelation functions of water molecule rotations were evaluated using standard methods.<sup>11</sup>

Direct evaluation of the energy barrier to diffusion was obtained by constraining the oxygen atom of a water molecule to remain close to a series of positions along a channel by adding a harmonic potential depending on the  $y$  coordinate. The system was then allowed to evolve freely after equilibration at a given temperature. Also, the barrier to crossing of the water molecules was derived by adding a harmonic potential constraining the component along  $y$  of the distance between the oxygen atoms of two molecules to oscillate close to a series of values and letting the system evolve along all other degrees of freedom.



TABLE III. Characteristic of the simulations performed in this work. The full hydrated crystal contains 72 molecules per simulation box. Partially dehydrated bikitaite was obtained by removing one or more molecule from each of the 9 channels. Among the properties, “structure” includes average positions of atoms, radial water–water,  $\text{Li}^+$ –water, and framework oxygen atoms–water distribution functions and interaction energies. MSD stands for mean square displacement of water molecule center of mass.

Number of water molecules	$T$ (K)	Duration (ns)	Evaluated properties
72	50	0.04	Structure
72	300	0.05	Structure, vibrational spectrum
72	316	1.2	Rotational relaxation time
72	424	1.2	Rotational relaxation time
72	615	1.2	Rotational relaxation time
72	800	0.45	Rotational relaxation time, MSD
63	479	2.1	Structure, MSD, cluster lifetime
63	889	4.7	Structure, MSD, cluster lifetime
54	614	3.3	Structure, MSD, cluster lifetime
54	835	3.3	Structure, MSD, cluster lifetime
36	680	6.0	Structure, MSD, cluster lifetime
36	1028	11.0	Structure, MSD, cluster lifetime
27	881	9.2	Structure, MSD
18	811	4.6	Structure, MSD
9	352	5.2	Structure, MSD,
			Distribution along the channels
9	651	5.2	Structure, MSD
			Distribution along the channels
9	761	5.0	Structure, MSD
			Distribution along the channels
9	898	10.6	Structure, MSD
			Distribution along the channels
2	300	$0.05 \times 12$	Crossing energy barrier
1	300	$0.05 \times 20$	Energy barrier to diffusion

### III. RESULTS AND DISCUSSION

#### A. Reproduction of experimental data and of CPMD simulations

The experimental knowledge of the behavior of water in bikitaite is given by neutron<sup>16</sup> and x-ray<sup>17</sup> diffraction structural data, completed by IR spectra<sup>17</sup> and NMR data,<sup>23</sup> inelastic incoherent neutron scattering (IINS),<sup>38</sup> and high-temperature x-ray diffraction.<sup>24,25</sup>

From neutron diffraction studies it appears that the libration motion of water molecules is relatively large even at low temperature (13 K) and, indeed, NMR experiments<sup>23</sup> evidenced that a flip motion of the water molecules already occurs at a relatively low temperature (224 K) with a correlation time of  $10^{-7}$  s. The NMR experiments were performed in the temperature range 224–418 K, detecting flip motion but no diffusion. The corresponding relaxation time follows closely an Arrhenius trend with values from  $10^{-7}$  s (224 K) to  $10^{-10}$  s (418 K). The fitted value of activation energy for the flip motion is  $30 \pm 2$  kJ/mol. The IR spectra were obtained by Quartieri *et al.*<sup>17</sup> using a microprobe, and it was possible to span only the frequency region including the bending and stretching modes of water molecules. In the low-frequency region of the vibrational spectrum (below  $1200 \text{ cm}^{-1}$ ), IINS spectra are available<sup>38</sup> which can probe the librational modes of water molecules and the  $\text{Li}^+$ –water or water–water stretch modes. High-temperature experiments were conducted by Vezzalini *et al.*<sup>24,25</sup> using synchrotron x-ray powder diffraction.

Overall, the water molecule chains embedded in bikitaite

show a high stability. CPMD studies by Fois *et al.*<sup>18</sup> demonstrated that these chains are stabilized by a permanent electric dipole parallel to the channel direction, which is coupled to an opposite dipole of the framework, stemming from a special arrangement of the aluminosilicate tetrahedra.

Previous CPMD simulations<sup>17</sup> reproduced well the experimental structure and vibrational spectrum of bikitaite, but, as their duration was limited to a few picoseconds due to their computational cost, were not sufficiently long for a quantitative study of the flip motion of water molecules, which shows relaxation times several order of magnitude longer.

In more recent CPMD studies by the same research group, the structure of bikitaite at high pressure<sup>20</sup> and the dehydration mechanism in the time range of 5–21 ps were performed.

Before undertaking long MD simulations using empirical functions for the interatomic interactions, intended as an extension of the CPMD ones, we verified that our model could reproduce the experimental structure (at different temperatures) and vibrational spectra, as well as CPMD results.

As it appears in Table IV, the structural properties computed using our model agree well with the experiment at low temperature (13 K for experiments, 50 K for simulations, in order to mimic approximately the average zero-point vibrational energy). At room temperature the flip motion of the water molecules causes the exchange of the hydrogen atoms, which in our simulations are clearly visible after some tens of picoseconds. Therefore, the hydrogen atom positions are

TABLE IV. Experimental (Ref. 14) and calculated coordinates at low temperature ( $\times 10^4$ ).

Atom	$x/a$		$y/b$		$z/c$	
	Expt.	Calc.	Expt.	Calc.	Expt.	Calc.
Si(11)	1062	1033	8651	8543	979	946
Si(12)	1038	1049	8006	8143	5049	5030
Al(13)	3801	3800	8778	8801	9377	9353
Al(21)	8991	8950	3650	3532	9073	9088
Si(22)	8917	8951	2991	3129	4878	4892
Si(23)	6195	6224	3773	3786	637	718
O(11)	2646	2575	7397	7163	569	436
O(12)	847	919	1883	1829	441	477
O(13)	1591	1607	8250	8051	3277	3223
O(14)	591	638	4842	5041	5208	5461
O(15)	2594	2567	9007	9443	6946	6932
O(16)	4508	4555	1960	1962	324	565
O(21)	7314	7311	2426	2153	9562	9691
O(22)	9275	9183	7050	7040	9695	9668
O(23)	8410	8366	3246	3032	6658	6662
O(24)	9344	9335	9843	10039	4618	4388
O(25)	7339	7411	4016	4410	2970	2966
O(26)	5589	5575	6823	6743	9778	9593
Li(1)	3117	3088	3667	3641	1506	1456
Li(2)	6977	6997	8692	8661	8691	8570
O(17)	4084	4095	3260	3076	4392	4595
H(11)	3194	3290	2991	3016	4825	5179
H(12)	4837	4748	1717	1395	4895	4954
O(27)	5988	5923	8253	8078	5830	5550
H(21)	6881	6856	8004	8022	5397	5170
H(22)	5252	5315	6691	6365	5330	5177

not well defined, corresponding to experimental temperature factors that are unusually large. In Fig. 2 the distributions of the hydrogen atoms coordinates are shown. They are bimodal, with maxima corresponding to the coordinates of different hydrogen atoms at low temperature.

The coordinates of the other atoms are similar to those at low temperature, and evenly close to the experimental values, and are reported in Table V along with those predicted by CPMD simulations.<sup>20</sup> Moreover, also the computed vibra-

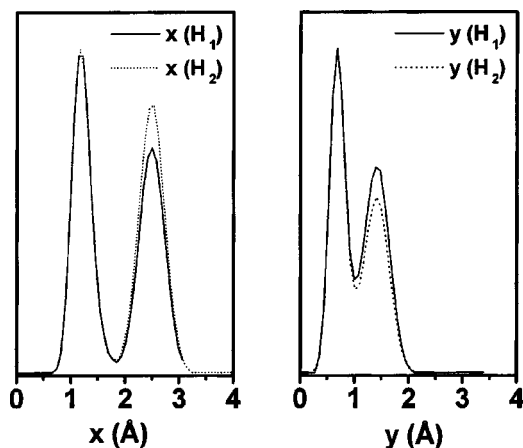


FIG. 2. Distribution function of the  $x$  and  $y$  coordinates of hydrogen atoms of water molecule of type 1. Continuous line:  $H_1$ ; dashed line:  $H_2$ . The distributions of the coordinates of molecule of type 2 (not shown) are similar. For the  $z$  coordinate no splitting is observed, as water molecules lie in the  $xy$  plane.

tional spectrum of the bending and stretching modes of water is satisfactory (see Fig. 3). We also evaluated the Fourier transforms of the motion of water hydrogen atoms, to derive a frequency spectrum, which is compared with the results of IINS experiments<sup>38</sup> in Table VI. It appears that also in this case the agreement is satisfactory.

Once the good quality of the potential model was ascertained, long time-scale simulations were performed in order to study the flip motion of the water molecules and the dehydration process. Following a well-established theory,<sup>39</sup> a quantitative comparison with NMR relaxation times is achieved by considering the second-order rotational correlation function

$$C_2(t) = \langle P_2[\mathbf{u}(0) \cdot \mathbf{u}(t)] \rangle, \quad (6)$$

where  $\mathbf{u}(t)$  is the unit vector of the HOH plane and  $P_2$  is the second-order Legendre polynomial.

Using Eq. (6), and assuming an exponential behavior of  $C_2(t)$ , the relaxation time for flip motion of water molecules  $\tau_2$  is evaluated by computing the time integral of  $C_2(t)$

$$\tau_2 = \int_0^\infty C_2(t) dt. \quad (7)$$

The computed values are compared with the experimental values in Table VII. They follow an Arrhenius trend, and the computed activation energy is 26 kJ/mol. Therefore, the simulated relaxation times are underestimated by about one order of magnitude, as the energy barrier is too low (the experimental one is  $30 \pm 2$  kJ/mol). However, problems arise when classical molecular dynamics is applied to systems where vibrations are present, as for solids and structured molecules. Indeed, for these kind of systems, as observed in Refs. 11 and 40, to obtain the same vibration amplitude of an oscillator predicted by quantum mechanics, the total energy of a corresponding classical oscillator must include the quantum zero-point energy that in quantum systems does not enter in the evaluation of the temperature. As an example, it is shown in Ref. 40 that the average zero-point vibrational amplitude at about 0 K for the atoms of a zeolite framework corresponds to a classical temperature of about 400 K! Therefore, for zeolites simulated using classical MD, the vibrational amplitude of the framework atoms and of the water molecules is underestimated, and the available space to flip motion is larger than in the case of the more realistic quantum system. These considerations could explain in part why the energy barrier to flip resulting from the classical MD simulations is smaller than the experimental one. Therefore, by including quantum corrections, the computed relaxation times could compare more favorably with experiment.

## B. Diffusion of water molecules and dehydration mechanism

As reported above, in the simulated fully hydrated system no diffusion was detected, even at the highest temperature (800 K). Therefore, in our model, the energy barriers to crossing of water molecules in the channels, an essential step to diffusion, in these conditions should be thermally inaccessible. In order to obtain a quantitative estimation, the energy

TABLE V. Experimental (Ref. 14) and calculated coordinates by CPMD (Ref. 20) and in this work at room temperature ( $\times 10^4$ ).

Atom	$x/a$			$y/b$			$z/c$		
	Expt.	CPMD	Calc.	Expt.	CPMD	Calc.	Expt.	CPMD	Calc.
Si(11)	1057	888	1033	8545	8186	8542	975	680	953
Si(12)	1038	854	1047	8006	8013	8143	5049	4793	5029
Al(13)	3803	3500	3798	8749	8515	8802	9374	9033	9353
Al(21)	8985	8730	8959	3639	3181	3530	9065	8854	9089
Si(22)	8920	8563	8948	2984	2972	3126	4877	4525	4895
Si(23)	6187	6000	6227	3748	3492	3788	630	473	722
O(11)	2641	2427	2577	7404	6978	7178	569	316	442
O(12)	830	577	916	1853	1463	1823	413	327	479
O(13)	1584	1365	1606	8261	7520	8045	3279	3005	3225
O(14)	557	231	620	4868	5134	5058	5173	5318	5455
O(15)	2612	2414	2569	8920	9245	9417	6947	6560	6932
O(16)	4496	4411	4552	1940	1616	1969	282	355	549
O(21)	7311	7020	7310	2433	2022	2166	9552	9372	9691
O(22)	9283	9016	9191	7021	6699	7033	9708	9377	9674
O(23)	8414	8065	8375	3281	2515	3024	6652	6370	6669
O(24)	9378	9173	9347	9872	10122	10060	4657	4016	4381
O(25)	7318	7047	7401	3929	4224	4390	2966	2675	2970
O(26)	5593	5217	5577	6797	6345	6748	9507	9289	9606
Li(1)	3095	2965	3081	3657	3307	3655	1469	1531	1428
Li(2)	6995	6648	6899	8665	8312	8680	8722	8256	8584
O(17)	4083	3951	4124	3224	2779	3076	4347	4472	4672
H(11)	3230	3186	3279	2849	2389	3187	4786	5052	5119
H(12)	4870	4695	4763	1784	1230	1541	4863	4807	5108
O(27)	5991	5634	5902	8225	7773	8068	5871	5357	5450
H(21)	6853	6439	6712	7872	7638	8856	5420	4792	5073
H(22)	5214	4995	5235	6763	6111	7126	5343	5012	5078

barrier to crossing was evaluated by following the procedure sketched in Sec. II. At room temperature, the energy barrier resulted to be 84 kJ/mol, too high to be overcome at a detectable rate in a MD simulation even by raising the temperature by any reasonable value. In the transition state configuration the oxygen atoms lie in a cross section of the channel also containing the Li(1) ion. Both the Li(1)–O and O–O average distances (0.198 and 0.250 nm, respectively) are shorter than the equilibrium values, and also the framework–water energy is repulsive. Therefore, the experimentally observed dehydration process above 375 K could be explained by considering that in real (finite) crystals water can escape

from the free ends of the channels, inducing a vacancy-driven stepwise diffusion, which eventually leads to dehydration, as experimentally observed.<sup>24,25</sup>

In order to verify this point, one, two, four, five, six, and seven water molecules were removed from each channel and for each concentration a series of simulations at different temperatures in the range 420–1000 K was performed (see Table III). The highest temperature is higher than that of the experimental full dehydration,<sup>24,25</sup> while the other temperatures are the ones corresponding approximately to experimental<sup>24,25</sup> equilibrium concentration of 7 (420 K), 6 (600 K), and 4 (620 K) water molecules per channel. The simulations with one molecule per channel were performed to evaluate the diffusion coefficient at high dilution and the energy barrier to diffusion. In order to study the diffusion mechanism, we considered first the trend of the mean square displacements (MSDs) of the oxygen atoms of the water molecules along the axis of the channels ( $y$  coordinate) as a function of time. They were analyzed by using log–log plots<sup>41</sup> in order to establish the power law of the time depen-

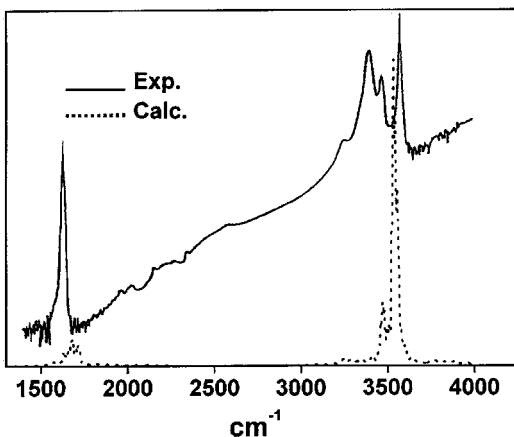


FIG. 3. Computed infrared spectrum of bikitaite, in arbitrary units, (dashed line) compared with experimental data (Ref. 15) (continuous line).

TABLE VI. Comparison between experimental inelastic incoherent neutron scattering (IINS) vibrational spectra and the power spectra of hydrogen atoms at 50 K. Values are given in  $\text{cm}^{-1}$ .

Modes	Li–water stretch	H–bond stretch	Libration	Libration
Calc. (this work)	.. <sup>a</sup>	165	320	540
Expt. (Ref. 38)	105	177	274	565

<sup>a</sup>Band not visible.

TABLE VII. Experimental (NMR) and calculated relaxation times  $\tau$  (in seconds) for the flip motion of water molecules in bikitaite at different temperatures.

$T$ (K)	316	424	611	800
Calc. (this work)	$1.7 \times 10^{-11}$	$2.3 \times 10^{-12}$	$2.6 \times 10^{-13}$	$6.0 \times 10^{-14}$
Expt. (Ref. 23)	$7 \pm 5 \times 10^{-10}$	$4 \pm 2 \times 10^{-11}$	$3 \pm 1 \times 10^{-12a}$	$7 \pm 2 \times 10^{-13a}$

<sup>a</sup>Extrapolated from the Arrhenius fit of the experimental data.

dence of MSD. Indeed, if it is assumed that the MSD depends on time as

$$\langle \mathbf{r}^2 \rangle = Ct^\alpha, \quad (8)$$

where  $C$  is constant, then  $\alpha$  is given by the slope of the logarithm of MSD vs the logarithm of time. If  $\alpha = 1$  ("normal" diffusion) the well-known Einstein formula can be used to estimate the diffusion coefficient. In the other cases the diffusivity can be characterized directly from the MSD trend. If  $\alpha \neq 1$  the diffusion process can be described by a generalized theory, often related to a continuous time random walk (CTRW) scheme, which is based on the hypothesis that the time intervals required for a diffusive jump do not follow a Gaussian distribution.<sup>42–45</sup> In particular, when the molecules cannot pass each other in the channels, single-file diffusion regime<sup>46–48</sup> is observed, entailing, for long but not infinite time,<sup>49</sup> a value  $\alpha = 0.5$ , and the MSD is given by

$$\langle \mathbf{r}^2 \rangle = 2F\sqrt{t}, \quad (9)$$

where  $F$  is the mobility factor of single-file diffusion.

The MSDs computed for the highest temperature in the usual way, by evaluating the MSDs of each molecule in the reference frame of the center of mass of the system and then averaging, are displayed in Fig. 4. While at full occupancy no diffusion occurs, by removing one or more water molecule per channel the MSDs increase monotonically against time, indicating that a diffusive process is present.

However, it clearly appears that the trend of MSDs is *not* linear. This is less evident for higher concentrations, but the derivatives of the log–log plots even in these cases are smaller than 1, although this value is reached and surpassed for short time intervals, but never maintained.

As for the MSDs not reported in Fig. 4, with 63 molecules in the simulation box at 480 K (approximately the experimental temperature corresponding to this equilibrium concentration), the diffusion is very slow, as about 1 nano-second is required for an average linear displacement of 0.25 nm, which is the distance between two adjacent equilibrium positions of the water molecules along the channels. Again, the trend vs time is not linear but, for the first 800 ps, the value of  $\alpha$  is close to 0.5. Only after 800 ps the MSD trend seems to become gradually linear.

By removing two molecules per channel the mobility of water molecules at corresponding temperatures is gradually increased, but the general trend remains the same at 614 K: for shorter times (till about 200 ps) the behavior of MSDs is close to that characteristic of single-file diffusion, and then gradually the linear trend seems to be approached.

A different situation is found when four molecules per channel, corresponding to one half of the full occupancy, are

removed. At 680 K, the log–log plot of the MSD shows three different slopes: for time shorter than about 14 ps the value of  $\alpha$  is close to 0.5, then it becomes about 0.75, and after 670 ps it reaches unity.

The value of  $\alpha$  close to 0.75 for large time intervals with four molecules per channel could not be easily explained, nor the even more irregular behavior of MSDs shown in Fig. 4, so we were drawn to examine the diffusive process in more detail, once the problem of the adequacy of the system size was discarded by considering a comparison with the CPMD simulations performed on a much smaller system and obtaining some dynamical quantities, such as the density profile along the channels, very similar to ours.

First, we had to ascertain that the molecules could not pass each other even in the presence of vacancies, in spite of the high energy barrier. Indeed, from the trend of MSDs it could be suggested that at the time scale of tens to hundreds of picoseconds, depending on the concentration of the defects, the diffusive process would be single file, but at longer times water molecules would begin to pass one another and a normal diffusion would be established. Even in a graphical animation of a water molecule chain obtained from the MD data (lasting some ps), besides evident flips of the water molecules around their axes, it seemed that one or two exchanges between adjacent water molecules occurred. We re-

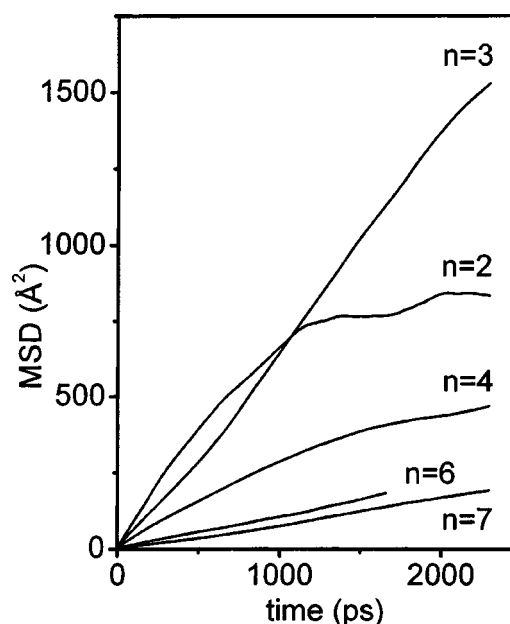


FIG. 4. Mean square displacements (MSDs) of water molecule center of mass in bikitaite, for different number of adsorbed molecules per channel ( $n$ ) and at the highest temperature for each concentration (see Table III).



call that, if exchanges are allowed, the diffusive process becomes “normal,” involving  $\alpha = 1$  in Eq. (8) as it was shown, for instance, in Ref. 50 for ethane in  $\text{AlPO}_4\text{-5}$  molecular sieve.

Therefore, a special, simple computer code was used to find these exchanges and none was detected in any trajectory at any temperature or concentration. Once it was demonstrated that the diffusion occurred in each channel exclusively as single-file process, we inspected a significant number of trajectories of single molecules and it appeared that the details of motion were rather complex. An example of these trajectories is illustrated in Fig. 5. At the picosecond scale [Fig. 5(a)] the molecules oscillate around the equilibrium positions, close to the Li cations, and eventually flip around the molecular axis by exchanging the hydrogen atoms. At a larger scale (tens to hundreds of picoseconds), as shown in Fig. 5(b), the diffusive jumps, usually between adjacent equilibrium positions, occur without a preferential direction and without crossing each other. When the trajectories are observed at the nanosecond scale [Fig. 5(c)], slow oscillations, whose amplitude is of the order of a nanometer, become evident. The observed behavior strictly recalls Fig. 8 of Ref. 49, where the trajectories of particles belonging to one-dimensional Lennard-Jones system in presence of background random noise are plotted. The trajectories of the water molecules hosted in the same channel are roughly parallel so that, as the trajectories evolve, a net shift of the center of mass of these molecules, always of the order of a nanometer or smaller, is observed [see Fig. 5(c)]. In different channels of the same system these shifts show a random direction and their average is very small (but not exactly zero), due to the conservation of the linear momentum of the whole system (water plus zeolite). The presence of an overall net shift in each channel on the considered time scale could explain the long-time behavior of most of the MSDs, approaching a slope close to 1 and mimicking a “quasnormal” diffusion.

From another viewpoint, the behavior of these trajectories can be considered as a shuttling motion of the water molecules, which favors the formation of clusters even at the highest temperature, because the molecules cannot pass one another. As for water in silicalite,<sup>14</sup> we evaluated the lifetime of the clusters, which is shorter than 1 picosecond for temperatures above 600 K. Contrary to the case of water in silicalite,<sup>14</sup> these lifetimes do not diminish for larger clusters, but are all similar, and the largest usually belongs to the largest cluster, because the clusters are formed by a ballistic effect of multiple collisions and not by attractive interactions as in silicalite.

It is important to remark that the systems considered in Refs. 46–49 to study the details of single-file diffusion, besides being one-dimensional, all have zero average linear momentum. However, as in our simulated system there are nine water molecule chains and the hosting zeolite framework, the average linear momentum of each chain, as above remarked, was not zero. Therefore, in order to compare the results of simulations of Refs. 46–49 with those of hydrated bikitaite, one should consider only one water molecule chain at a time, and evaluate the MSDs with respect to the center of mass of the chain.

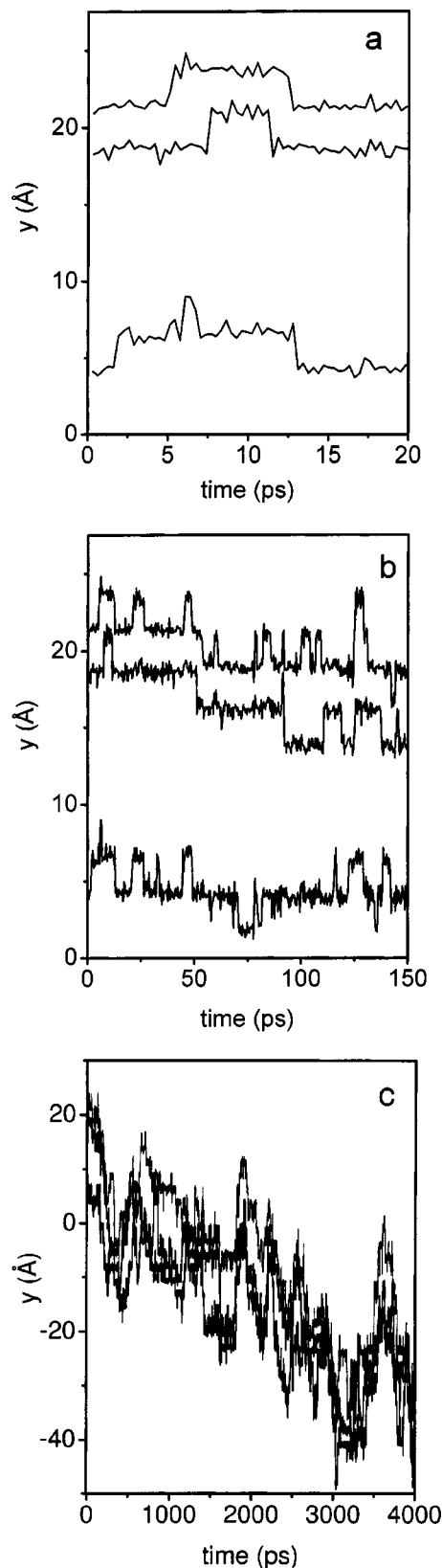


FIG. 5. Trajectories of the centers of mass of three water molecules adsorbed in a channel at 881 K at different time scales. (a): tens of picoseconds; (b): hundreds of picoseconds; (c): nanoseconds.

This procedure stems from the general principles of mechanics, stating that it is always possible to separate the motion of the center of mass of a system from that considered with respect to the center-of-mass reference frame (CM



frame), which can be seen also as “internal” or relative motion of the molecules of the chain. In particular, for the case of anomalous diffusion, the problem was treated by Metzler *et al.*<sup>44</sup>

Thus, we evaluated the MSDs for the molecules adsorbed in the same channel in the reference frame of the center of mass of these molecules (the internal MSDs) and then we averaged over the channels to improve the statistics. In more detail, the procedure is the following. Let  $\mathbf{r}_i(t)$  be the position of the center of mass (c.o.m.) of the  $i$ th water molecule with respect to the c.o.m. of the simulated system along the channel axis at time  $t$ . Then the c.o.m. of the molecules adsorbed in the  $k$ th channel are

$$\bar{\mathbf{r}}_k(t) = \frac{1}{M_k} \sum_{i \in C_k} m_i \mathbf{r}_i(t) \quad (k=1, \dots, n_k), \quad (10)$$

where  $C_k$  is the set of the molecules adsorbed in the  $k$ th channel  $M_k = \sum_{i \in C_k} m_i$  is their total mass,  $m_i$  is the mass of a water molecule, and  $n_k$  is the number of the channels. Therefore, the coordinates with respect to the c.o.m. of the  $k$ th channel are

$$\mathbf{r}_i^k(t) = \mathbf{r}_i(t) - \bar{\mathbf{r}}_k(t) \quad (k=1, \dots, n_k, i \in C_k). \quad (11)$$

With respect to this coordinate system, the total linear momentum of the molecules adsorbed in the  $k$ th channel is zero

$$\mathbf{P}_k(t) = \sum_{j \in C_k} m_j \dot{\mathbf{r}}_j^k(t) = \sum_{j \in C_k} \left[ m_j \dot{\mathbf{r}}_j^k(t) - \frac{m_j}{M_k} \sum_{i \in C_k} m_i \dot{\mathbf{r}}_i(t) \right] = \mathbf{0} \quad (k=1, \dots, n_k). \quad (12)$$

The MSD of the water molecules adsorbed in the  $k$ th channel evaluated with respect to the c.o.m. of the same channel is given by

$$\langle |\mathbf{r}^k(t)|^2 \rangle = \frac{1}{N_k} \sum_{i \in C_k} \langle |\mathbf{r}_i^k(t)|^2 \rangle \quad (k=1, \dots, n_k), \quad (13)$$

where  $N_k$  is the number of water molecules adsorbed in the  $k$ th channel and the single-particle MSDs  $\langle (\mathbf{r}_i^k)^2 \rangle$  are computed, as usual, as averages over independent time origins.

Finally, an average of MSDs is taken over the channels to improve the statistics

$$\langle |\mathbf{r}(t)|^2 \rangle_C = \frac{1}{n_k} \sum_k \langle |\mathbf{r}^k(t)|^2 \rangle. \quad (14)$$

This procedure was not necessary in the previous simulation studies of single-file diffusion in molecular sieves, which did not include explicitly the total initial zero momentum condition. For instance, in those performed by Sholl *et al.*,<sup>51–53</sup> the diffusion of relatively short-lived clusters was studied by MD at low temperature for at most 20 ps (Ref. 52), and the coarse-grained dynamical simulations of microsecond time scale reported in Ref. 53 implicitly assume total initial zero momentum condition. In Ref. 14 we observed single-file-like diffusion of water in silicalite at very low temperature (below 160 K) with respect to the c.o.m. of the simulated system because in these cases the temperature was so low that the diffusion occurred through an exchange of

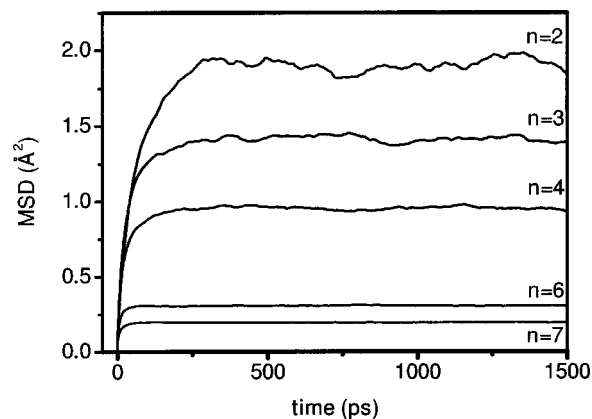


FIG. 6. Mean square displacement (MSDs) of water molecule center of mass in bikitaite, as evaluated with respect to the reference frame of the center of mass of the molecules adsorbed in the same channel, for different number of adsorbed molecules per channel ( $n$ ) and at the highest temperature for each concentration (see Table III).

molecules between frozen clusters, which were nested in the channel and therefore practically at rest with respect to the framework and to the c.o.m. of the system.

As shown in Fig. 6, the trend of the MSDs computed with respect to the c.o.m. of the molecules adsorbed in the channels changes completely and becomes similar to that reported in Fig. 1 of Ref. 49: after a short time, the MSDs reach a maximum and oscillate around a constant small value. In Ref. 41 reduced units are used, but an approximated correspondence with the units adopted in the present work can be estimated.

Indeed, although water molecules are not spherical, one may assume approximately the hydrogen bond energy (8 kJ/mol) as a measure of the interaction and the  $y$  component of the O–O distance (0.247 nm) as the diameter of the “rods” and the reduced unit of length  $l^*$ , so that the reduced units of time and of temperature become  $t^* = 0.37$  ps and  $T^* = 940$  K, which is fortuitously close to the highest temperatures of our simulations.

By comparing Fig. 1 of Ref. 41 (relative to a concentration close to that of our system with 7 molecules per channel) and Fig. 6 of this paper, it appears that the crossover time between the single-file behavior and oscillatory, time-independent long-time behavior is similar and is surprisingly small, especially if compared with the results of Ref. 53, where the crossover time is larger than tens of microseconds. This seemingly striking difference is explained below.

Moreover, one must take into account that the high temperature favors frequent collisions and, in the case of our system, the diffusion is strongly hindered by the interactions between water molecules and Li ions. This hindered motion reduces the amplitudes of the MSDs along the axis of the channels in the long-time limit,  $\langle y^2 \rangle_\infty$ , with respect to that found in Ref. 49 for a one-dimensional system of Lennard-Jones rods diffusing without friction. Moreover, we verified that the computed amplitudes are of the same order of magnitude but smaller than those expected from a simplified theory reported by Hahn and Kärger,<sup>46</sup> who showed that, for a periodic system of  $N$  hard rods with period  $L$  and linear

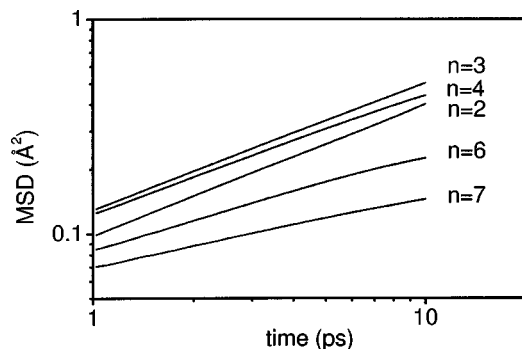


FIG. 7. Log-log plot of the mean square displacements (MSDs) displayed in Fig. 6 at short time scale.

concentration  $\theta$  diffusing without friction,  $\langle y^2 \rangle_\infty$  is given by a temperature-independent formula

$$\langle y^2 \rangle_\infty = \frac{1}{6} \frac{N-1}{N} L^2 (1-\theta)^2, \quad (15)$$

where  $N$  is the number of particles contained in a one-dimensional periodic cell of length  $L$  and  $\theta$  is the relative concentration.

The likeness of Fig. 6 with Fig. 1 of Ref. 49 is not a proof of that in bikitaite the relative motion of the water molecules follows a single-file mechanism, unless the MSD's trend is observed at short-time intervals and with a log-log scale. This is done in Fig. 7, where it appears doubtless that for all concentration the value of  $\alpha$  is indeed close to 0.5 until 10 ps. Then, at longer times for smaller concentrations,  $\alpha$  begins to decrease and finally oscillates around zero.

According to Ref. 49, an estimate of the crossover time between the single-file behavior and oscillatory, time-independent long-time behavior,  $t_{\text{cross}}$ , can be approximated by

$$t_{\text{cross}} \approx \frac{N}{12D_{\text{short}}} \left( \frac{1}{\theta} - 1 \right)^2 l^2, \quad (16)$$

where  $D_{\text{short}}$  is the diffusion coefficient of the molecules in the time interval between collisions,  $l$  is the particle dimension, and the other symbols are the same as in Eq. (15). The right-hand side of Eq. (16) contains an  $l^2$  term which was not included in Ref. 49 because reduced units were adopted there, so that  $l=1$ . Taking the values of  $t_{\text{cross}}$  from the simulations, the resulting values are of  $D_{\text{short}}$ , the same order of magnitude of the diffusion coefficients obtained at infinite dilution.

Indeed, at infinite dilution, which can be simulated with one molecule per channel as in our model, no interaction is present between periodic images of the particles and the interactions between molecules adsorbed in different channels are negligible, the diffusive process becomes "normal," and it is possible to evaluate a diffusion coefficient in the usual way. This was done for bikitaite at four different temperatures, and we obtained:  $D(352 \text{ K}) = 0.99 \cdot 10^{-10} \text{ m}^2 \text{ s}^{-1}$  (nearly two orders of magnitude smaller than the value for bulk water at the same temperature),  $D(651 \text{ K}) = 1.69 \cdot 10^{-9} \text{ m}^2 \text{ s}^{-1}$ ,  $D(761 \text{ K}) = 2.90 \cdot 10^{-9} \text{ m}^2 \text{ s}^{-1}$ ,

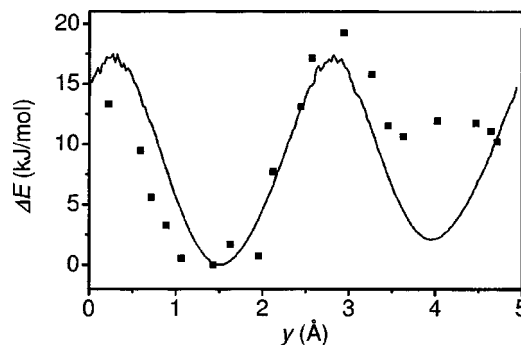


FIG. 8. Energy profile along a channel for a molecule diffusing at 351 K as derived from Eq. (12) (continuous line) and differential potential energy computed directly at 300 K as reported in Sec. II (filled squares). The  $y$  coordinates of Li cations are 1.83 and 4.15 Å.

$D(898 \text{ K}) = 4.91 \cdot 10^{-9} \text{ m}^2 \text{ s}^{-1}$ . They follow strictly an Arrhenius trend, and the activation energy to diffusion obtained from the Arrhenius equation is  $18.6 \pm 0.4 \text{ kJ/mol}$ . There are at least two other methods to derive this quantity, along with more details of the potential energy of the molecules moving in the channels: by means of the density profile along the channels and, directly, by constraining the oxygen atom of a water molecule to remain close to a series of positions along a channel.

According to the Boltzmann distribution (in the last decade it has been shown that molecules adsorbed in a vibrating framework behave as a small canonical ensemble; see Ref. 11) the density profile of a molecule moving along a channel is given by

$$\rho(y) = A \exp \left[ - \frac{\Delta E(y)}{k_B T} \right], \quad (17)$$

where  $A$  is a normalizing constant,  $\Delta E(y)$  is the total energy of the particle (including kinetic energy) along the channel axis, evaluated with respect to the minimum energy,  $k_B$  is the Boltzmann constant, and  $T$  is the temperature. The density profile can be evaluated from the simulation data, and using Eq. (17)  $\Delta E(y)$  is easily derived. In Fig. 8 the density profile is reported for the simulation at 351 K along with the values of the corresponding potential energy evaluated directly in a series of points along  $y$  as briefly reported in Sec. II. The agreement is only fair, but, besides the remark that the two quantities are not equivalent, because  $\Delta E(y)$  includes the average translational energy at the top of the barrier  $E_t = \frac{1}{2} k_B T$ , which is not possessed by the particles constrained in a stated point along  $y$ , it should be reminded that the energy surface by a moving particle for a sufficiently long time is much better sampled than for a single partially hindered particle. However, taking into account the correction for  $E_t$ , the resulting energy barrier derived from the density profile is  $18.9 \text{ kJ/mol}$  (moreover, the same value results from the same method applied to the simulations at higher temperatures) and that obtained from the direct method is  $18.5 \text{ kJ/mol}$ , a good agreement, nicely consistent with the value computed from the Arrhenius equation ( $18.6 \pm 0.4 \text{ kJ/mol}$ ).

With these data in mind, we can come back to the different order of magnitude of crossover times between the

single-file behavior and oscillatory, time-independent long-time behavior. Indeed, assuming that the diffusion coefficients follow the Arrhenius law down to low temperatures, and estimating the crossover time from Eq. (16), one obtains a value of  $t_{\text{cross}}$  of the order of nanosecond at 200 K and of the order of  $10^8$  ps at 100 K, thus reaching a value similar to those reported in Ref. 53. Thus, the large change of  $t_{\text{cross}}$  is caused by the strong temperature dependence of the diffusion coefficients because of the relatively large activation energy to diffusion.

In Fig. 8 also an asymmetry of the energy profile is evident, as the two Li cations are not in equivalent positions. This finding is in agreement with the experimental result<sup>24,25</sup> that during the dehydration the preferred position of the water molecules is close to the Li(1) position, corresponding to the absolute minimum on the left in Fig. 8.

The direct evaluation of the energy barrier was performed also by Ceriani *et al.*,<sup>21</sup> who reported a barrier of about 30 kJ/mol. This apparent discrepancy with our results deserves a short comment. We also found one energy minimum, deeper than that reported in Fig. 8 in correspondence to the Li(1) position, raising the barrier to about 29 kJ/mol, but this minimum is very narrow and separated from the other one by a thermally inaccessible barrier, as they were obtained by starting from slightly different positions and orientations of the water molecule. Possibly in the CPMD calculations only the deeper minimum was found, and certainly in our simulations without constraints the diffusing molecules prefer a path from which the deeper minimum is not easily reachable.

The deeper minimum corresponds to a configuration in which the whole water molecule lies roughly in a cross section of the channel (whereas usually one OH bond is directed along the channel axis) and the Li cation is closer to the framework than usual when hydrated. Indeed, when water molecules are removed and diffuse, Li cations temporarily lose the coordination to four oxygen atoms (three of the framework and one of the nearest water molecule) characteristic of the fully hydrated system, and become free to approach the three oxygen atoms of the framework. Their original position is restored when a water molecule passes at a close distance from a cation. Therefore, Li cations shuttle between two equilibrium positions when water molecules are diffusing. This phenomenon was observed experimentally,<sup>24,25</sup> as well in CPMD<sup>21</sup> and our simulations. The displacement, occurring along the *c* axis, is large (about 0, 15 nm) and is evidenced by a bimodal distribution of the Li cations distribution function.

In the simulation of hydrated silicalite<sup>14</sup> we observed that at high temperature the water molecules could rotate almost freely. In partially dehydrated bikitaite the nearly free rotation of the molecules is confirmed, among others, by the trend of the intermolecular energies between water molecules (see Fig. 9). Taking into account that for our model the energy of one hydrogen bond (HB) is about 8 kJ/mol, from Fig. 9 it is evident that, when more than one molecule per channel is removed, less than one HB per molecule is formed, on average.

For the fully hydrated system, a change of slope at about

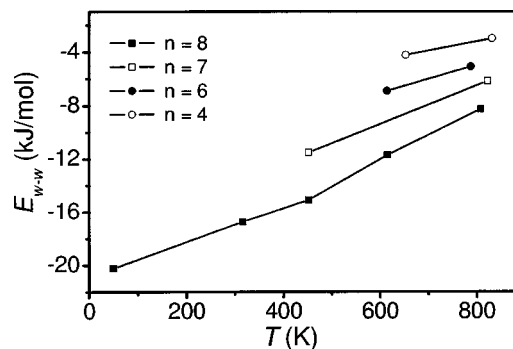


FIG. 9. Intermolecular average potential energy of water in bikitaite, as a function of temperature and of the number of water molecule per channel (*n*).

420 K is observed in Fig. 9. This change corresponds to an intermolecular energy of 16 kJ/mol, that is to the energy of two HBs per molecule, characteristic of the low-temperature structure. By raising the temperature, one of the HBs of an increasing number of molecules gradually is broken by the rotational motion until, at 800 K, only one HB per molecule, on average, remains.

#### IV. CONCLUSIONS

In this work classical MD simulations are used to study the dynamical behavior of water adsorbed in bikitaite at the nanosecond time scale. New empirical potentials for the Li<sup>+</sup>-water and Li<sup>+</sup>-framework interactions were derived, yielding a good reproduction of both available experimental data and Car-Parrinello simulation results. The extended time scale permitted the study of the rotational relaxation times, which compare fairly with the experiments.

The simulation of the diffusive process of the adsorbed water molecules, which at reasonable temperatures occurs only if a partial dehydration is present, evidenced a complex mechanism. In the present work it was outlined and partially explained as a single-file diffusion superimposed to a random collective shuttling of the water molecules adsorbed in the channels. However, when studied in the reference frame of the center of mass of the molecules adsorbed in the same channel, the single-file mechanism becomes evident and can be investigated in detail. Further studies are in progress to better understand this mechanism, in particular from the viewpoint of CTRW theory.<sup>42-45</sup>

Meanwhile, we are studying an analogous system, the Li-ABW zeolite,<sup>54,55</sup> which as bikitaite contains Li cations and water molecule linear chains adsorbed in straight channels. A comparison between the two related systems could help in understanding more details of the dynamical behavior of water molecular chains and, in general, of single-file diffusion mechanism in real systems.

#### ACKNOWLEDGMENTS

This research is supported by Ministero dell'Istruzione, dell'Università, e della Ricerca (MIUR) by Università degli studi di Sassari and by Istituto Nazionale per la Scienza e Tecnologia dei Materiali (INSTM), which are acknowledged.

The authors are grateful to Professor Fois and Professor Quartieri for providing the preprints of Refs. 21 and 25 before publication.

- <sup>1</sup>M. A. Ricci and M. Rovere, *J. Phys.* IV **10**, 187 (2000).
- <sup>2</sup>M. A. Ricci, F. Bruni, P. Gallo, M. Rovere, and A. K. Soper, *J. Phys.: Condens. Matter* **12**, A345 (2000).
- <sup>3</sup>R. Bergman and J. Swenson, *Nature (London)* **403**, 283 (2000).
- <sup>4</sup>R. Bergman, J. Swenson, L. Börjesson, and P. Jacobsson, *J. Chem. Phys.* **113**, 357 (2000).
- <sup>5</sup>J. Swenson, R. Bergman, and W. S. Howells, *J. Chem. Phys.* **113**, 2873 (2000).
- <sup>6</sup>J. Swenson, R. Bergman, and S. Longeville, *J. Chem. Phys.* **115**, 11299 (2001).
- <sup>7</sup>T. H. Truskett, P. G. Debenedetti, and S. Torquato, *J. Chem. Phys.* **114**, 2401 (2001).
- <sup>8</sup>A. Giaya and S. W. Thompson, *J. Chem. Phys.* **116**, 2565 (2002); T. H. Truskett, P. G. Debenedetti, and S. Torquato, *ibid.* **117**, 8162 (2002); A. Giaya and S. W. Thompson, *ibid.* **117**, 8264 (2002).
- <sup>9</sup>A. Giaya and S. W. Thompson, *J. Chem. Phys.* **117**, 3464 (2002).
- <sup>10</sup>*Computer Simulations in Chemical Physics*, edited by M. P. Allen and D. J. Tildesley (Kluwer, Dordrecht, 1994).
- <sup>11</sup>P. Demontis and G. B. Suffritti, *Chem. Rev.* **97**, 2845 (1997).
- <sup>12</sup>P. Cicu, P. Demontis, S. Spanu, G. B. Suffritti, and A. Tilocca, *J. Chem. Phys.* **112**, 8267 (2000).
- <sup>13</sup>P. Demontis, G. Stara, and G. B. Suffritti, in *Studies in Surface Science and Catalysis*, 142, edited by A. Aiello, G. Giordano, and F. Testa (Elsevier, Amsterdam, 2002), p. 1931.
- <sup>14</sup>P. Demontis, G. Stara, and G. B. Suffritti, *J. Phys. Chem. B* **107**, 4426 (2003).
- <sup>15</sup>K. Koga, *J. Chem. Phys.* **116**, 10882 (2002).
- <sup>16</sup>K. Stahl, A. Kvik, and S. Ghose, *Zeolites* **9**, 303 (1989).
- <sup>17</sup>S. Quartieri, G. Vezzalini, A. Sani, E. Galli, E. S. Fois, A. Gamba, and G. Tabacchi, *Micro. Meso. Mater.* **30**, 77 (1999).
- <sup>18</sup>E. Fois, G. Tabacchi, S. Quartieri, and G. Vezzalini, *J. Chem. Phys.* **111**, 355 (1999).
- <sup>19</sup>E. Fois, A. Gamba, G. Tabacchi, S. Quartieri, and G. Vezzalini, *J. Phys. Chem. B* **105**, 3012 (2001).
- <sup>20</sup>O. Ferro, S. Quartieri, G. Vezzalini, E. Fois, A. Gamba, and G. Tabacchi, *Am. Mineral.* **87**, 1415 (2002).
- <sup>21</sup>C. Ceriani, E. Fois, A. Gamba, G. Tabacchi, O. Ferro, S. Quartieri, and G. Vezzalini, *Am. Mineral.* **89**, 102 (2004).
- <sup>22</sup>R. Car and M. Parrinello, *Phys. Rev. Lett.* **55**, 2471 (1985).
- <sup>23</sup>K. Larsson, J. Tegenfeldt, and Å. Kvik, *J. Phys. Chem. Solids* **50**, 107 (1989).
- <sup>24</sup>G. Vezzalini, O. Ferro, S. Quartieri, A. F. Gualtieri, G. Cruciani, E. Fois, C. Ceriani, and A. Gamba in *13th International Zeolite Conference, Recent Research Reports* (Groupe Français des Zéolithes, Paris, 2001), 09-R-04.
- <sup>25</sup>O. Ferro, S. Quartieri, G. Vezzalini, C. Ceriani, E. Fois, A. Gamba, and G. Cruciani, *Am. Mineral.* **89**, 94 (2004).
- <sup>26</sup>W. P. Kraemer, B. O. Roos, and P. E. M. Siegbahn, *Chem. Phys.* **69**, 305 (1982).
- <sup>27</sup>P. Demontis, E. S. Fois, A. Gamba, and G. B. Suffritti, *Chem. Phys. Lett.* **127**, 456 (1986).
- <sup>28</sup>P. Demontis, G. B. Suffritti, S. Bordiga, and R. Buzzoni, *J. Chem. Soc., Faraday Trans.* **91**, 525 (1995).
- <sup>29</sup>A. P. Lyubartsev, K. Laasonen, and A. Laasonen, *J. Chem. Phys.* **114**, 3120 (2001).
- <sup>30</sup>K. Hermansson and I. Olovsson, *Theor. Chim. Acta* **64**, 265 (1984).
- <sup>31</sup>P. Demontis, G. B. Suffritti, E. S. Fois, A. Gamba, and G. Morosi, *Mater. Chem. Phys.* **29**, 357 (1991).
- <sup>32</sup>B. Roux and M. Karplus, *J. Comput. Chem.* **16**, 690 (1995).
- <sup>33</sup>E. D. Glendening and D. Feller, *J. Phys. Chem.* **99**, 3060 (1995).
- <sup>34</sup>X. Periole, D. Allouche, J.-P. Daudey, and Y.-H. Sanejouand, *J. Phys. Chem. B* **101**, 5018 (1997).
- <sup>35</sup>G. Artioli, J. V. Smith, and Å. Kvik, *Acta Crystallogr., Sect. C: Cryst. Struct. Commun.* **40**, 1658 (1984).
- <sup>36</sup>D. Wolf, P. Keblinski, S. R. Phillpot, and J. Eggebrecht, *J. Chem. Phys.* **110**, 8254 (1999).
- <sup>37</sup>P. Demontis, S. Spanu, and G. B. Suffritti, *J. Chem. Phys.* **114**, 7980 (2001).
- <sup>38</sup>C. M. B. Line and G. J. Kearley, *J. Chem. Phys.* **112**, 9058 (2000).
- <sup>39</sup>R. G. Gordon, in *Advances in Magnetic Resonance*, edited by J. S. Waugh (Academic New York, 1968), Vol. 3, p. 1.
- <sup>40</sup>H. Jobic, K. Smirnov, and D. Bougeard, *Chem. Phys. Lett.* **344**, 147 (2001).
- <sup>41</sup>S. El Amrani and M. Kolb, *J. Chem. Phys.* **98**, 1509 (1993).
- <sup>42</sup>E. W. Montroll and G. H. Weiss, *J. Math. Phys.* **10**, 753 (1969).
- <sup>43</sup>V. Balakrishnan, *Physica A* **132**, 569 (1985).
- <sup>44</sup>R. Metzler, J. Klafter, and I. M. Sokolov, *Phys. Rev. E* **58**, 1621 (1998).
- <sup>45</sup>R. Metzler and J. Klafter, *Phys. Rep.* **339**, 1 (2000).
- <sup>46</sup>K. Hahn and J. Kärger, *J. Phys. Chem.* **100**, 316 (1996).
- <sup>47</sup>D. Keffer, A. V. McCormick, and H. T. Davis, *Mol. Phys.* **87**, 367 (1996).
- <sup>48</sup>K. K. Mon and J. K. Percus, *J. Chem. Phys.* **117**, 2289 (2002).
- <sup>49</sup>S. Pal, G. Srinivas, S. Bhattacharyya, and B. Bagchi, *J. Chem. Phys.* **116**, 5941 (2002).
- <sup>50</sup>P. Demontis, J. Gulín González, G. B. Suffritti, and A. Tilocca, *J. Am. Chem. Soc.* **123**, 5069 (2001).
- <sup>51</sup>D. S. Sholl and K. A. Fichtorn, *Phys. Rev. Lett.* **79**, 3569 (1997).
- <sup>52</sup>D. S. Sholl, *Chem. Phys. Lett.* **305**, 269 (1999).
- <sup>53</sup>D. S. Sholl and C. Kun Lee, *J. Chem. Phys.* **112**, 817 (2000).
- <sup>54</sup>E. Krogh Andersen and G. Plough-Sørensen, *Z. Kristallogr.* **176**, 67 (1986).
- <sup>55</sup>P. Norby, A. Nørlund Chistensen, and E. Krogh Andersen, *Acta Chem. Scand., Ser. A* **A40**, 500 (1986).